https://doi.org/10.15407/ujpe70.9.588

A. JUMABAEV,[1] H. HUSHVAKTOV,[1] A. ABSANOV,[1] B. KHUDAYKULOV,[1]
U. HOLIKULOV,[1] L. DJUMANOV,[1] N. ISSAOUI,[2] L. BULAVIN[3]

[1] Department of Optics and Spectroscopy, Samarkand State University
(15, University Blvd., 140104 Samarkand, Uzbekistan; e-mail: abduvakhidj@gmail.com)
[2] Laboratory of Quantum and Statistical Physics, University Monastir
(Monastir 5079, Tunisia)
[3] Department of Molecular Physics, Taras Shevchenko National University of Kyiv,
(4, Academician Glushkov Ave., Kyiv 03680, Ukraine)

EXPERIMENTAL AND THEORETICAL INVESTIGATION OF INTERMOLECULAR INTERACTIONS IN NITROMETHANE AND ITS SOLUTIONS

The present work discusses the vibrational (Raman and IR) spectra of nitromethane and its solutions in polar (chloroform) and nonpolar solvents (carbon tetrachloride, hexane). The geometries, Mulliken charge distribution, molecular electrostatic potential surface, and frontier molecular orbitals of nitromethane complexes with chloroform molecules $CH_3NO_2 + n \cdot CHCl_3$ ($n = 1$–3) are analyzed using density functional theory (DFT) with the B3LYP/6-311++G(d,p) basis set. Weak molecular interactions in complexes are investigated using Atoms in Molecule (AIM) analysis.

Keywords: nitromethane, Raman spectra, hydrogen bond, DFT, AIM.

1. Introduction

Hydrogen bonding, as a special type of intermolecular interaction, plays an important role in controlling the structure and physicochemical properties of biomolecular systems [1–5]. Its manifestation in vibrational spectra has not been fully explained to date and has been the focus of attention for researchers for many years. The vibrational spectra of substances in the gas phase give a wide range of information about hydrogen bonding. However, the present models do not provide enough information for the liquid state. As a result, the possibility of obtaining more data in the study of intermolecular interactions in liquids using Raman spectroscopy provides an increasing need for scientific research in this field.

Nitro compounds are important classes of compounds widely used in chemical synthesis, pharmacology, electrochemistry, as organic solvents, and as fuel additives [6–8]. Nitro alkanes have the chemical formula R-NO_2 and have a high dipole moment of 3.5–4.0 Debye, so they have a relatively high boiling point [9].

Nitromethane (CH_3NO_2) is one of the simplest nitro compounds and is liquid in its normal state. This substance is very versatile; it is not only a simple

Citation: Jumabaev A., Hushvaktov H., Absanov A., Khudaykulov B., Holikulov U., Djumanov L., Issaoui N., Bulavin L. Experimental and theoretical investigation of intermolecular interactions in nitromethane and its solutions. *Ukr. J. Phys.* **70**, No. 9, 588 (2025). https://doi.org/10.15407/ujpe70.9.588.

solvent used for the purification process and reaction medium but also an intermediate in the organic synthesis of various chemicals. In addition, nitromethane is known for its explosive properties; it burns easily and is used as fuel. Due to its high performance and low toxicity, it is known as a stored monopropellant with prospects for use in space propulsion [10]. Several experimental and theoretical studies have been carried out to understand the intermolecular interactions of liquid nitromethane. X-ray and neutron diffraction were used to observe the structure of liquid nitromethane, with simulations by Car-Parrinello [11]. In addition, there are several molecular simulation studies [12–14], but the detailed description of the liquid structure is still unclear.

D. Roy and A. Kovalenko [6] used 3D-RISM-KH and DFT-D3 methods to study the liquid states of nitromethane, nitroethane, and nitrobenzene. Similarly, Seigo Hayaki *et al.* [9] used the reference interaction site model (RISM) and MP2 theories to understand the structure of nitromethane liquid.

In several theoretical studies [10, 15–17], intermolecular interactions in nitromethane dimers and trimers were studied using theoretical methods, and the most stable complexes were presented. In these studies, it was reported that nitromethane dimers and trimers are formed by intermolecular dipole-dipole interaction and weak hydrogen bonding.

By analyzing the literature, it was found that the detailed description of the structure of liquid nitromethane is still unclear, including information on how a deeper understanding of intermolecular interactions in nitromethane can lead to advancements in fields such as chemical synthesis, pharmacology, and fuel additives can emphasize the practical implications of the study. In this study, the intermolecular interactions in liquid nitromethane solutions in hexane (C_6H_{14}) and chloroform ($CHCl_3$) were discussed using Raman spectroscopy. At the same time, the optimal geometry, bond energies, and Raman spectra of molecular complexes formed by nitromethane with chloroform were determined using density functional theory (DFT) methods. In order to understand non-covalent interactions and solvent effects, Mulliken atomic charges, molecular electrostatic potential (MEP), frontier molecular orbitals (FMO), and Atoms in Molecule (AIM) analyses were performed.

2. Experimental and Computational Details

Raman spectra of pure liquid nitromethane and its binary solutions in hexane and chloroform at different concentrations were recorded on a Renishaw Invia Raman spectrometer at room temperature. An argon laser with a wavelength of 785 nm and a power equal to 100 mW and a diffraction grating with a period of 1200 lines/mm were used as a source of excitation light. A standard Renishaw CCD camera detector was used to record the scattered light.

All computations were performed in the Gaussian 09W package program [18]. The geometry of nitromethane and its complexes formed with chloroform molecules was optimized by Density Functional Theory (DFT) in the B3LYP set of functions. The 6-311++G(d,p) basis set, which includes diffuse and polarization functions, was used in the calculations to account for hydrogen bonding as accurately as possible. In addition, for a deeper understanding of intermolecular interactions, topological features of the electron density distribution in the most stable structure based on the AIM theory were obtained using the MULTIWFN [19] software.

3. Results and Discussion

3.1. Vibrational Analysis

Figure 1 shows the Raman spectrum of pure liquid nitromethane in the range of 0–4000 cm^{-1}. It can be seen that relatively high-intensity spectral bands are located between 500 cm^{-1} and 3200 cm^{-1}. One important spectral line in this range corresponds to a weak peak at 654 cm^{-1}, which is assigned to the $\delta(NO_2)$ bending vibration. The spectral lines at 475 cm^{-1} and 603 cm^{-1} correspond to the $r(NO_2)$ rocking and $\omega(NO_2)$ wagging vibrations, respectively. Additionally, spectral bands composed of combinations of C–H stretching and bending vibrations appear in the region of 1100–1500 cm^{-1}.

Polarized and non-polarized Raman spectra of pure nitromethane and its solutions in hexane and chloroform were obtained for further analysis. Figure 2 presents the isotropic and anisotropic Raman components of pure liquid nitromethane in the 600–700 cm^{-1} range:

$$I_{\text{iso}} = I_{\parallel} - \frac{4}{3} I_{\perp}, \quad I_{\text{aniso}} = I_{\perp},$$

where $I_{\parallel}$ and $I_{\perp}$ are the polarized and non-polarized Raman components, respectively. The spectral band

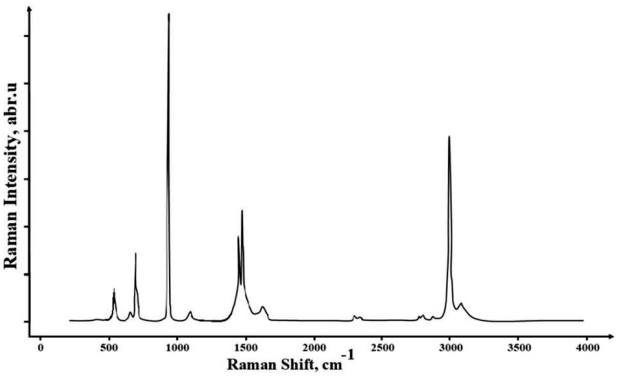

Fig. 1. Experimental Raman spectrum of pure liquid nitromethane in the range of 0–4000 cm^{-1}

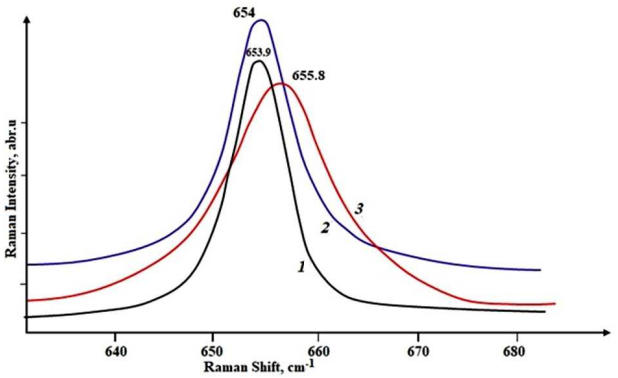

Fig. 2. Parallel (*1*), anisotropic (perpendicular) (*2*), and isotropic components of the Raman spectra of pure liquid nitromethane in the 600–700 cm^{-1} range (*3*)

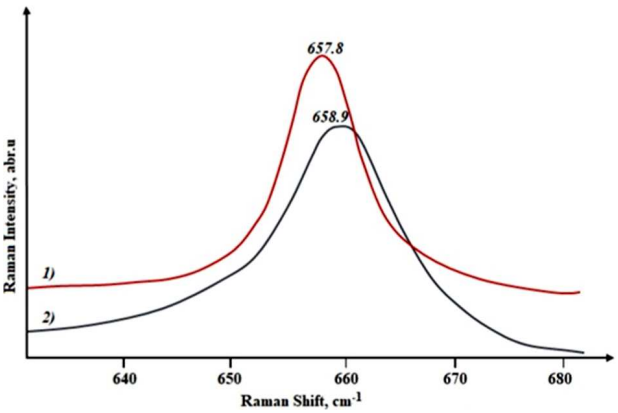

Fig. 3. Raman spectra of a nitromethane-hexane solution in the range of 600–700 cm^{-1}: $I_{\parallel}$ (parallel) (*1*) and $I_{\perp}$ (perpendicular) components (*2*)

in this region corresponds to the $\delta(NO_2)$ bending vibration of nitromethane. It can be observed that the maximum wavenumbers of these spectral bands do not coincide, exhibiting asymmetry on the low-frequency side and a relatively broad half-width.

Raman spectra of a nitromethane-hexane solution with a concentration of 0.4÷0.6 mole fraction are shown in Fig. 3. It can be seen from the picture that the maximum wave number of the band corresponding to the vibration of the $\delta(NO_2)$ band of pure nitromethane corresponds to 654 cm^{-1}, and in its solution in hexane, this band shifts to approximately ≈658 cm^{-1}. Both in pure nitromethane and in its hexane solution, the maximum wave numbers of the isotropic and anisotropic components do not coincide. In pure nitromethane, the difference between these maximum wave numbers is about ≈2 cm^{-1}. This difference is ≈1 cm^{-1} in the solution of nitromethane with hexane at a concentration of 0.4÷0.6 mole fraction.

The main reason for this is that nitromethane molecules have a large dipole moment, and therefore high-energy dipole-dipole interactions can be observed [15]. In the presence of a non-polar solvent, the interaction energy between nitromethane molecules should be greater than the interaction energy with solvent molecules. As the interaction between oriented molecules decreases, the vibrational frequency also decreases, reducing the difference between the maxima of the parallel and perpendicular components of the Raman spectra. The decrease in this frequency difference leads to a reduction in the half-width of the isotropic band. Two possible reasons for this effect include a reduction in the number of vibrational states during exposure processes or a change in resonance energy transfer. This should lead to changes in the polarizability tensor and bond force constants.

We present the results of an analysis of Raman spectra and a comparison of the infrared absorption spectra of liquid nitromethane in the region of 600–3500 cm^{-1}, where there are several vibrational bands with a complex structure (Fig. 4). A number of small frequencies of mutual and joint vibrations appear in the Raman spectra. An experimental study was conducted to investigate the behavior of pure nitromethane and its solutions with CCl_4 and chloroform, aiming to analyze the effects of different solvents on the vibrational spectra.

Vibrations of liquid nitromethane molecules appear in the vibrational spectra in the form of several peaks corresponding to different types of vibrations, such as stretching and bending. Raman spectra of pure liquid nitromethane provide valuable insights into the distinctive characteristics of molecular vibrations and rotations.

In the Raman spectra of vibrations of the CNO group of nitromethane molecules, intermolecular bonding is clearly evident (Fig. 4).

For nitromethane solutions in CCl_4 (Fig. 4), an increase in intensity and a shift of the spectral band to higher frequencies are observed. This suggests that molecular complexes of nitromethane are prominently present in the solution, as CCl_4 is a neutral solvent.

In the Raman spectra of the vibrations of the C–N–O group of nitromethane molecules, intermolecular bonding is clearly evident (Fig 4).

In solutions of nitromethane with CCl_4 (Fig. 4), the intensity increases, and the band imperceptibly shifts to the high-frequency side. This means that molecular complexes of nitromethane are noticeably contained in this solution, since CCl_4 is a neutral solvent.

In a solution with chloroform in the experiment, we have a significant change in the band under study. The Raman spectra clearly show bands at 1377 cm^{-1} and 1400 cm^{-1}, corresponding to the vibrations of the NO_2 group, as well as at 2966 cm^{-1}, which refers to the symmetrical stretching of the CH_3 group vibrations of nitromethane molecules (Fig. 4).

The band with a frequency of 3026 cm^{-1} belongs to the vibrations of the CH group in the molecule, and this band is clearly visible in the spectra related to low nitromethane content in a solution with chloroform (Fig. 4).

As the nitromethane content in the solution decreases, the intensity of this band decreases, which means nitromethane molecules form complexes with chloroform molecules. Analysis of the change in the band at 1377 cm^{-1} and 1400 cm^{-1}, corresponding to vibrations of the NO_2 group shows that this group actively participates in intermolecular interaction and therefore the group stretches. This statement is confirmed by an increase in the intensity of the band with a frequency of 640 cm^{-1} and 955 cm^{-1} corresponding to small vibrations of the NO_2 group.

Each peak in the spectrum corresponds to a certain vibrational energy of the molecule. Analysis of these peaks makes it possible to determine the frequencies

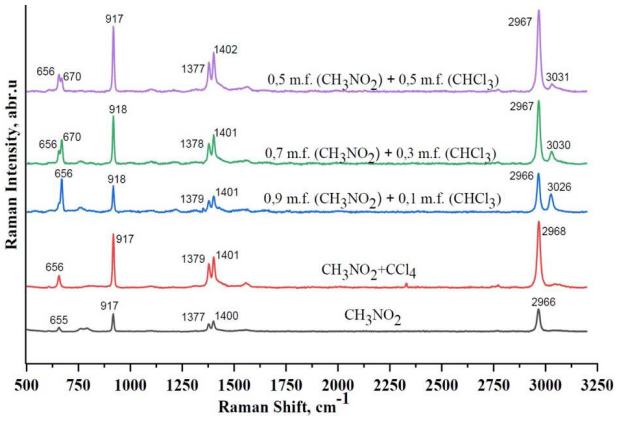

Fig. 4. Raman spectra of nitromethane (CH_3NO_2) and its solutions in carbon tetrachloride (CCl_4) and chloroform ($CHCl_3$)

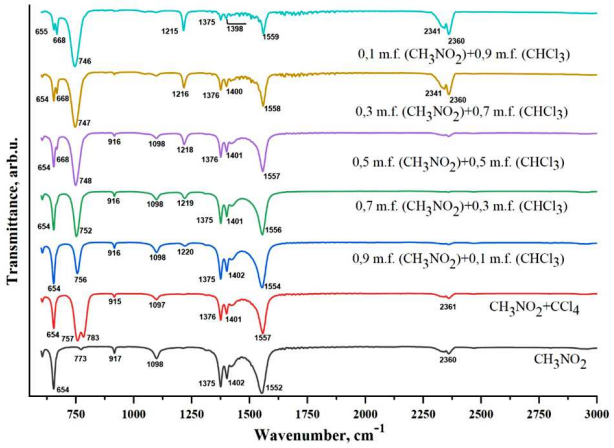

Fig. 5. FT-IR spectra of nitromethane (CH_3NO_2) and its solutions in carbon tetrachloride (CCl_4) and chloroform ($CHCl_3$)

and amplitudes of vibrations, which in turn provides information about the chemical structure and properties of liquid nitromethane.

Our statements on the analysis of Raman spectra are confirmed by the infrared absorption spectra of pure liquid nitromethane and in solutions with CCl_4 and chloroform in the region of 600–3500 cm^{-1} (Fig. 5).

The infrared absorption spectrum of liquid nitromethane typically includes several characteristic peaks that correspond to vibrational and/or rotational modes of the molecule. Typically contains bands corresponding to different chemical bonds in the molecule. Some of them may be associated with stretching vibrations C–H, N–H, C–N, C=O and other functional groups. The specific peak values will

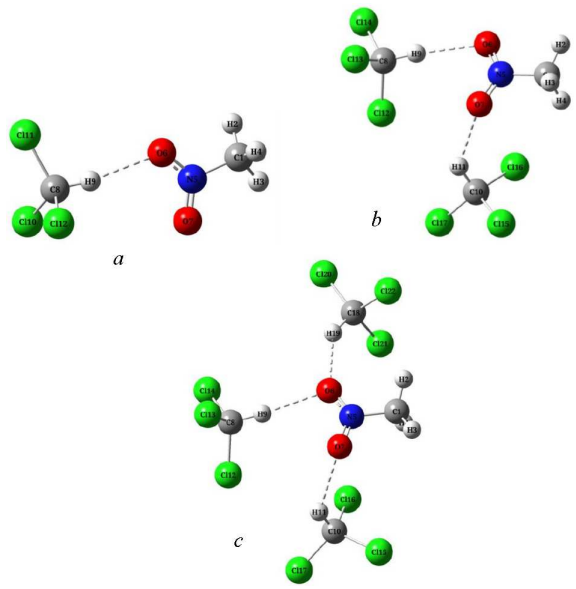

Fig. 6. Optimal geometries of complexes of nitromethane with chloroform molecules

depend on the specific temperature, pressure, and purity of the sample.

Expanding on the comparison between the Raman spectra of pure nitromethane and its solutions with hexane, carbon tetra chloride, and chloroform can offer insights into how the solvent environment influences the vibrational frequencies and spectral characteristics. By examining the differences in peak shifts, intensities, and band structures across various solutions, a more comprehensive interpretation of the molecular interactions can be derived.

The infrared absorption spectra of solutions of nitromethane with chloroform will differ from the spectra of pure nitromethane due to the interaction of nitromethane molecules with chloroform molecules. This interaction resulted in an intensity increase of the band at 773 cm^{-1}, with a shift towards lower frequencies by 25 cm^{-1}. In CCl_4 solutions, the band shifts to higher frequencies by 10 cm^{-1} and splits into two bands at 767 cm^{-1} and 783 cm^{-1}. In solutions with chloroform, a new band appears with a frequency of 1220 cm^{-1}, corresponding to vibrations of molecular aggregates of nitromethane and chloroform molecules. This band noticeably shifts with an increase in the molar fraction of chloroform in the solution, and the experiment also observed a change in the intensity of the band with a frequency of 2341 cm^{-1} and 2380 cm^{-1}, corresponding to the CH vibrations of nitromethane.

These spectrum shifts may result from intermolecular interactions such as hydrogen bonding and dipole-dipole interactions, which influence the vibrational behavior of the molecules in solutions. Hence, the spectra of nitromethane solutions with chloroform offer valuable insights into the precise nature of interactions between these compounds, enhancing the understanding of their chemical behavior.

The analysis of Raman spectra not only aids in identifying compounds in solution but also facilitates the evaluation of their conformation and structural arrangements. Therefore, examining the Raman spectra of liquid nitromethane in various solutions with chloroform yields crucial insights into the chemical and physical characteristics of the system.

3.2. Geometric analysis

Calculations in the gas and solvent phases were performed using the DFT: B3LYP/6-311+G(d,p) set of functions to investigate the intermolecular interactions in solutions and the formation mechanism of 1 : 1, 1 : 2, and 1 : 3 systems of CH_3NO_2–$CHCl_3$. Figure 6 shows the optimal geometric structures of nitromethane complexes with chloroform molecules. Calculation results showed the presence of a weak N=O···H–C hydrogen bond between the nitro (NO_2) group of nitromethane and the C–H group of chloroform.

Intermolecular interactions lead to alterations in the geometric parameters of molecules, the redistribution of charges among atoms, and modifications in vibration spectra. Table 1 presents the calculated geometric parameters (bond lengths and angles) of nitromethane and its complexes formed with chloroform molecules in the gas and solvent phases.

It can be seen from the table that the length of the N=O of the nitromethane molecule increases compared to the gas phase under the influence of the solvent environment by a specific amount. Also, the C–N=O increases. On the other hand, the length of the C–N bond and the value of the O=N=O angle decrease.

In the formation of the $CH_3NO_2 + CHCl_3$ heterodimer, the length of the O_6–N_5 bond participating in the hydrogen bond increases by 0.0046 Å (in the gas phase) and 0.0049 Å(in the solvent phase)

Table 1. **Geometrical parameters of $CH_3NO_2 + n \cdot CHCl_3$ ($n = 0$–3) complexes**

Bonds	CH_3NO_2		CH_3NO_2+$CHCl_3$		CH_3NO_2+2$CHCl_3$		CH_3NO_2+3$CHCl_3$	
	Gas	Solvent	Gas	Solvent	Gas	Solvent	Gas	Solvent
Bond length, Å								
O^7-N^5	1.2209	1.2226	1.2180	1.2203	1.2232	1.2197	1.2220	1.2232
O^6-N^5	1.2209	1.2226	1.2255	1.2265	1.2238	1.2261	1.2269	1.2238
N^5-C^1	1.5035	1.5009	1.5016	1.4991	1.4995	1.4988	1.4972	1.4978
H^4-C^1	1.0900	1.0900	1.0898	1.0896	1.0900	1.0901	1.0895	1.0900
H^3-C^1	1.0863	1.0856	1.0855	1.0878	1.0851	1.0855	1.0847	1.0851
H^2-C^1	1.0863	1.0856	1.0871	1.0852	1.0862	1.0869	1.0865	1.0862
Bond angle, Degree								
C^1-N^5-O^6	117.1612	117.6387	116.6701	117.1729	118.0244	117.4935	117.5062	118.0244
C^1-N^5-O^7	117.1612	117.6387	118.0233	118.2888	117.0605	118.0070	118.3724	117.0605
O^6-N^5-O^7	125.6520	124.7010	125.2299	124.5237	124.9064	124.4835	124.1093	124.9064
H^2-C^1-H^3	112.9328	112.9134	112.8526	112.8264	112.7202	112.9575	112.8406	112.7202
H^2-C^1-H^4	110.5560	110.6828	110.0494	110.2569	111.8336	110.3637	110.2350	111.8336
H^2-C^1-N^5	107.9973	107.9319	107.6238	107.6559	108.2234	107.7445	107.6696	108.2234
H^3-C^1-H^4	110.5560	110.6828	111.2957	111.2292	109.9458	111.0651	111.3605	109.9458
H^3-C^1-N^5	107.9973	107.9319	108.1214	108.0972	107.3791	108.0417	108.0062	107.3791
H^4-C^1-N^5	106.5279	106.4067	106.6510	106.4834	106.4452	106.3658	106.4267	106.4452

compared to the monomer state. The length of the O_7–N_5 bond, which does not participate in hydrogen bonding, is slightly reduced. C–H and C–N bond lengths are almost unchanged. In the formation of $CH_3NO_2 + 2 \cdot CHCl_3$ and $CH_3NO_2 + 3 \cdot CHCl_3$ complexes, the O_6–N_5 bond length increases from 1.2209 Å (1.2226 Å in the solvent phase) to 1.2225 Å (1.2238 Å in the solvent phase) and 1.2261 Å (1.2276 Å in the solvent phase), respectively.

Similarly, the O_7–N_5 bond length increases from 1.2209 Å (1.2226 Å in the solvent phase) to 1.2222 Å (1.2232 Å in the solvent phase) and 1.2197 Å (1.2202 Å in the solvent phase), respectively.

Intermolecular interaction energies in $CH_3NO_2 + + CHCl_3$, $CH_3NO_2 + 2 \cdot CHCl_3$, and $CH_3NO_2 + + 3 \cdot CHCl_3$ complexes in the gas phase are 3.14, 6.06, and 8.57 kcal/mol, respectively. Similarly, in the solvent phase, these energies are 2.06, 3.74, and 5.18 kcal/mol, respectively.

The length of the C_8–$H_9 \cdots O_6$ hydrogen bond in the $CH_3NO_2 + CHCl_3$ complex is 2.25 Å. In the $CH_3NO_2 + 2 \cdot CHCl_3$ complex, the C_8–$H_9 \cdots O_6$ and C_{10}–$H_{11} \cdots O_7$ hydrogen bond lengths are 2.30 Å and 2.36 Å, respectively.

For the $CH_3NO_2 + 3 \cdot CHCl_3$ complex, the hydrogen bond lengths are as follows: C_8–$H_9 \cdots O_6 = = 2.33$ Å, C_{18}–$H_{19} \cdots O_6 = 2.36$ Å, and C_{10}–$H_{11} \cdots O_7 = 2.46$ Å.

3.3. Mulliken atomic charge analysis

Table 2 shows the distribution of electron density in nitromethane and its complexes with chloroform molecules.

The table indicates that all hydrogen atoms in the nitromethane molecule are positively charged, while carbon, nitrogen, and oxygen atoms are negatively charged. During the formation of the complex, the electron density of nitrogen and oxygen atoms changes significantly. In the solvent phase, the amount of charge on hydrogen atoms increases, and the amount of charge on other atoms decreases.

3.4. Molecular electrostatic potential surface (MEPS) analysis

The molecular electrostatic potential surface (MEPS) analysis is widely used to visually understand the physicochemical properties of molecular systems, such as charge density, relative polarity, size, shape,

Table 2. **Mulliken atomic charges of $CH_3NO_2 + n{\cdot}CHCl_3$ (n = 0–3) complexes**

Atoms	CH_3NO_2		$CH_3NO_2 + CHCl_3$		$CH_3NO_2 + 2CHCl_3$		$CH_3NO_2 + 3CHCl_3$	
	Gas	Solvent	Gas	Solvent	Gas	Solvent	Gas	Solvent
1 C	–0.3020	–0.2982	–0.2994	–0.2964	–0.3348	–0.3114	–0.4041	–0.3723
2 H	0.1808	0.1903	0.1879	0.1965	0.1849	0.1981	0.2105	0.2129
3 H	0.1808	0.1903	0.1833	0.1901	0.1974	0.1948	0.1960	0.2014
4 H	0.1964	0.2152	0.2013	0.2176	0.2120	0.2231	0.2304	0.2362
5 N	–0.1171	–0.0782	–0.1815	–0.1504	–0.2325	–0.2124	–0.2646	–0.2236
6 O	–0.0694	–0.1097	–0.0315	–0.0588	0.0028	–0.0305	0.0347	–0.0207
7 O	–0.0694	–0.1097	–0.0347	–0.0690	0.0169	–0.0355	0.0231	0.0057

Table 3. **Selected important quantum chemical parameters of nitromethane**

Parameters, eV	Gas	$CHCl_3$	CCl_4	C_6H_{14}
E_{HOMO}	–8.546	–8.636	–8.598	–8.587
E_{LUMO}	–2.455	–2.548	–2.514	–2.502
E_g	6.091	6.088	6.084	6.085
η	3.045	3.044	3.042	3.042
μ	–5.500	–5.592	–5.556	–5.544
ω	4.967	5.136	5.074	5.052
IE	8.546	8.636	8.598	8.587
EA	2.455	2.548	2.514	2.502

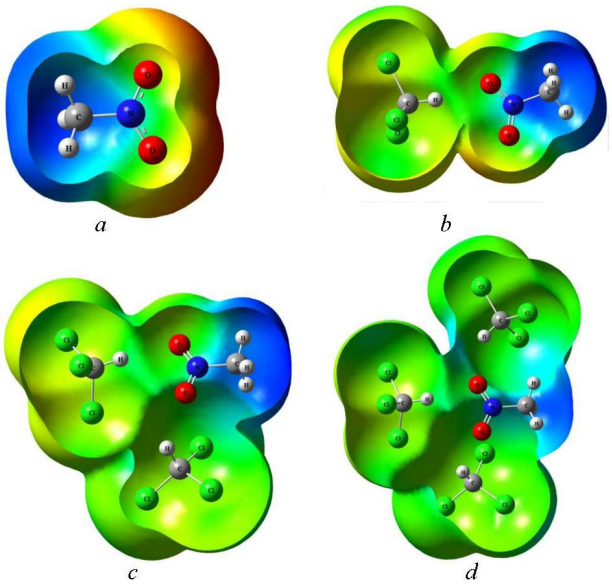

Fig. 7. MEPS of nitromethane (*a*) and its molecular complexes with chloroform molecules (*b*, *c*, *d*)

and chemical reactivity site [20, 21]. In addition, MEPS analysis helps identify electrophilic and nucleophilic regions to study intermolecular interactions, particularly intermolecular hydrogen bonding.

The MEP of nitromethane and its complexes with chloroform molecules were calculated using the B3LYP/6-311++G(d,p) method and are shown in Figure 7. The blue regions, representing high electrostatic potential energy, are prominently located above the hydrogen atoms of nitromethane.

Usually, the level of electrostatic potential is represented by different colors. The color code of nitromethane MEPS is between -4.329×10^{-2} a.u. to $\times 10^{-2}$ a.u. Red indicates the lowest electrostatic potential energy and blue indicates the highest electrostatic potential energy. Intermediate potentials are given by colors in the following sequence: red < orange < yellow < green < blue. They are strong regions for nucleophilic attacks. Red regions are observed above oxygen atoms, which are strong regions for electrophilic attacks.

3.5. Frontier molecular orbital (FMO) analysis

The interaction of a molecule with other molecules can be approximated by the highest occupied molecular orbital (HOMO) and the lowest unoccupied molecular orbital (LUMO). The frontier orbital gap is the energy difference between the HOMO and the LUMO. This is an important indicator that characterizes the kinetic stability and chemical reactivity of the molecule. A small frontier orbital gap means that the molecule is polarizable, reactive and a soft molecule, while a large frontier orbital gap means a

Table 4. **Topological parameters of $CH_3NO_2 + n \cdot CHCl_3$ (n = 1–3) complexes**

Complexes	H-bonds	$\rho(r)$	$G(r)$	$V(r)$	$H(r)$	$\nabla^2\rho(r)$	E_{HB} (kcal/mol)
$CH_3NO_2 + CHCl_3$	C^8–H^9...O^6	0.0142	0.0102	–0.0085	0.0016	0.0473	2.67
$CH_3NO_2 + 2 \cdot CHCl_3$	C^8–H^9...O^6	0.0139	0.0100	–0.0083	0.0017	0.0470	2.60
	C^{10}–H^{11}...O^7	0.0114	0.0086	–0.0069	0.0017	0.0415	2.16
$CH_3NO_2 + 3 \cdot CHCl_3$	C^8–H^9...O^6	0.0139	0.0099	–0.0083	0.0015	0.0457	2.60
	C^{18}–H^{19}...O^6	0.0119	0.0088	–0.0072	0.0016	0.0416	2.26
	C^{10}–H^{11}...O^7	0.0091	0.0068	–0.0055	0.0013	0.0326	2.13

rigid molecule. Frontier molecular orbitals are important for optical and electrical properties. LUMO represents the ability to accept electrons and HOMO indicates the ability to donate electrons as an electron donor [22]. Figure 8 shows HOMO and LUMO maps of nitromethane in gas, chloroform, carbon tetrachloride and hexane phases.

Global descriptors such as energy gap, chemical hardness, chemical potential, global electrophilicity index, electron affinity and ionization potential can be determined using HOMO and LUMO energies:

- energy gap: $E_g = E_{\text{HOMO}} - E_{\text{LUMO}}$;
- chemical hardness: $\eta = \frac{E_{\text{HOMO}} - E_{\text{LUMO}}}{2}$;
- chemical potential: $\mu = \frac{E_{\text{HOMO}} + E_{\text{LUMO}}}{2}$;
- global electrophilicity index: $\omega = \frac{\mu^2}{2\eta}$;
- electron affinity: $\text{EA} = -E_{\text{LUMO}}$;
- ionization potential: $\text{IP} = -E_{\text{HOMO}}$.

Table 3 presents some important quantum-chemical parameters of the nitromethane molecule calculated in different phases. A large energy gap or a large hardness value indicates a hard molecule, a small energy gap or a large softness value indicates a soft molecule. The electrophilic index of a molecule provides information about the ability of a compound to bind to biomolecules. A high electrophilic index value indicates the molecule's strong binding capacity with biomolecules, making it an electrophilic species. At the same time, a low value of chemical hardness with a high negative value of chemical potential means that the studied molecule is a soft molecule with high polarizability.

The calculated HOMO energy values are −8.546, −8.636, −8.598, and −8.587 eV in gas, chloroform, carbon tetrachloride, and hexane, respectively. The corresponding LUMO values are −2.455, −2.548, −2.514, and −2.502 eV. The energy gap (E_g) values between HOMO and LUMO are 6.091, 6.088, 6.084, and 6.085 eV in gas, chloroform, carbon tetrachloride, and hexane, respectively.

3.6. Atoms in Molecule (AIM) analysis

Atoms in Molecule (AIM) analysis, based on Bader's theory [19], is widely used to describe various noncovalent interactions in molecular systems, particularly hydrogen bonding [23, 24]. Due to the spatial concentration of electrons, bond critical points (BCPs) appear between atoms. Topological parameters such as electron density $\rho(r)$, Laplacian electron density $\nabla^2\rho(r)$, energy density $H(r)$, Lagrangian kinetic energy density $G(r)$, and potential energy density $V(r)$

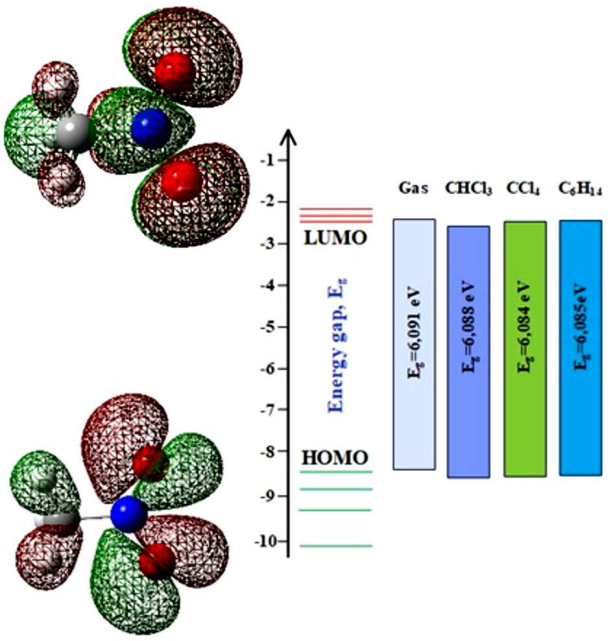

Fig. 8. HOMO and LUMO maps of nitromethane in different phases

in BCPs characterize the nature of hydrogen bonding. Here $H(r) = G(r) + V(r)$. Rozas *et al.* [25] classified hydrogen bonding as follows:

• $\nabla^2\rho(r) > 0$, $H(r) > 0$, and $E_{\text{HB}} < 12$ kcal/mol – weak hydrogen bonding;

• $\nabla^2\rho(r) > 0$, $H(r) < 0$, and $12 < E_{\text{HB}} < 24$ kcal/mol – medium hydrogen bonding;

• $\nabla^2\rho(r) < 0$, $H(r) < 0$, and $E_{\text{HB}} > 24$ kcal/mol – strong hydrogen bonding.

The hydrogen bond energy was determined using the formula: $E_{\text{HB}} = V(r)/2$ [26]. If the energy density at critical points is negative ($H(r) < 0$), the hydrogen bond has a covalent character, whereas a positive value ($H(r) > 0$) indicates an electrostatic character.

Figure 7 illustrates the presence of critical points along the C–H···O bond path in $CH_3NO_2 + n \cdot CHCl_3$ (n = 1–3) complexes, indicating significant intermolecular interactions.

Table 4 presents the topological parameters at the critical points of the complexes. It can be seen from the table that the electron density and Laplacian of the electron density at the critical points of the bond are in the range of 0.0091−0.0142 au and 0.0326−0.473 au, respectively. These values are in the hydrogen bond range of of 0.0033−0.168 au and 0.020−0.139 au, respectively. All Laplacian of the electron density and energy densities at critical points of hydrogen bonding have positive values. It characterizes that all hydrogen bonds are electrostatic in nature. It can be seen from the table that the hydrogen bond energies in the complexes are in the range of 2.13−2.67 kcal/mol and mean weak hydrogen bonds.

4. Conclusion

The isotropic and anisotropic components of the Raman spectra of the $\delta(NO_2)$ vibration of liquid nitromethane do not match. In a mixture of nitromethane and hexane, this band is shifted to a higher frequency. The main reason for this is that hexane molecules have the ability to break various molecular aggregations in nitromethane. In the chloroform solution of nitromethane, it is found that the Raman spectra of $\delta_s(CH_3)$ bending and $v_s(NO_2)$ stretching vibration bands shift toward the lower frequency. Quantum-chemical calculations confirm that nitromethane and chloroform molecules form molecular complexes with the dipole-dipole interactions and weak hydrogen bonds of the C–H···O type.

This work was supported by Project no. FZ-20200929385, Ministry of Higher Education, Science and Innovation of the Republic of Uzbekistan.

1. *Hydrogen Bonding–New Insight*. Edited by S.J. Grabowski (Springer, 2006).
2. G.A. Pitsevich, E.N. Kozlovskaya, A.E. Malevich, I.Yu. Doroshenko, V.S. Satsunkevich, Lars G.M. Pettersson. Some useful correlations for H-bonded systems. *Mol. Cryst. Liq. Cryst.* **696** (1), 15 (2020).
3. H.A. Hushvaktov, F.H. Tukhvatullin, A. Jumabaev, U.N. Tashkenbaev, A.A. Absanov, B.G. Hudoyberdiev, B. Kuyliev. Raman spectra and *ab initio* calculation of a structure of aqueous solutions of methanol. *J. Mol. Struct.* **1131**, 25 (2017).
4. U. Holikulov, M. Khodiev, N. Issaoui, A. Jumabaev, N. Kumar, O.M. Al-Dossary. Exploring the non-covalent interactions, vibrational and electronic properties of 2-methyl-4-hydro-1,3,4-triazol-thione-5 in different solutions. *J. King Saud Univ. Sci.* **2024**, 103164 (2024).
5. A. Jumabaev, H. Hushvaktov, B. Khudaykulov, A. Absanov, M. Onuk, I. Doroshenko, L. Bulavin. Formation of hydrogen bonds and vibrational processes in dimethyl sulfoxide and its aqueous solutions: Raman spectroscopy and ab initio calculations. *Ukr. J. Phys.* **68** (6), 375 (2023).
6. D. Roy, A. Kovalenko. A 3D-RISM-KH study of liquid nitromethane, nitroethane, and nitrobenzene as solvents. *J. Mol. Liq.* **332**, 115857 (2021).
7. T. Litzinger, M. Colket, M. Kahandawala, S.-Y. Lee, D. Liscinsky, K. McNesby, R. Pawlik, M. Roquemore, R. Santoro, S. Sidhu, S. Stouffer. Fuel additive effects on soot across a suite of laboratory devices, part 2: Nitroalkanes. *Combust. Sci. Technol.* **183**, 739 (2011).
8. A. Jumabaev, H. Hushvaktov, A. Absanov, I. Doroshenko, B. Khudaykulov. Experimental and computational analysis of CN and C–H stretching bands in acetonitrile solutions. *Fizyka Nyzkykh Temperatur* **51** (2), 224 (2025).
9. S. Hayaki, H. Sato, Sh. Sakaki. A theoretical study of the liquid structure of nitromethane with RISM method. *J. Mol. Liq.* **377**, 9 (2009).
10. L. Min-Joo, K. Ji-Young. A theoretical study on the intermolecular hydrogen bond between nitromethanes and the stabilization of nitromethane dimer. *J. Korean Chem. Soc.* **48**, 229 (2004).
11. T. Megyes, S. Bálint, T. Grósz, T. Radnai, I. Bakó. The structure of aqueous sodium hydroxide solutions: A combined solution x-ray diffraction and simulation study. *J. Chem. Phys.* **128**, 164507 (2008).
12. J.M. Seminario, M.C. Concha, P. Politzer. Structure of liquid nitromethane: Comparison of simulation and diffraction studies. *J. Chem. Phys.* **126**, 164507 (2007).
13. H.E. Alper, F. Abu-Awwad, P. Politzer. Molecular dynamics simulations of liquid nitromethane. *J. Phys. Chem. B* **103**, 9738 (1999).

14. D.C. Sorescu, B.M. Rice, D.L. Thompson. Theoretical studies of solid nitromethane. *J. Phys. Chem. B* **104**, 8406 (2000).
15. L. Jin-Shan, Z. Feng, J. Fu-qiang. An *ab Initio* study of intermolecular interactions of nitromethane dimer and nitromethane trimer. *J. Comput. Chem.* **24** (3), 345 (2003).
16. L. Jin-Shan, X. He-Ming, D. Hai-Shan. A theoretical study on the intermolecular interaction of energetic system–Nitromethane dimer. *Chin. J. Chem.* **18**, 815 (2000).
17. A. Jumabaev, H. Hushvaktov, I. Doroshenko, A. Absanov, G. Sharifov. Role of intermolecular interactions in formation of molecular clusters in liquid nitromethane and its solutions. *Mol. Cryst. Liq. Cryst.* **749**, 132 (2000).
18. M.J. Frisch, G.W. Trucks, H.B. Schlegel, G.E. Scuseria, M.A. Robb, J.R. Cheeseman, G. Scalmani, V. Barone, B. Mennucci, G.A. Petersson, H. Nakatsuji, M. Caricato, X. Li, H.P. Hratchian, A.F. Izmaylov, J. Bloino, G. Zheng, J.L. Sonnenberg, M. Hada, M. Ehara, K. Toyota, R. Fukuda, J. Hasegawa, M. Ishida, T. Nakajima, Y. Honda, O. Kitao, H. Nakai, T. Vreven, J.A. Montgomery, Jr., J.E. Peralta, F. Ogliaro, M. Bearpark, J.J. Heyd, E. Brothers, K.N. Kudin, V.N. Staroverov, R. Kobayashi, J. Normand, K. Raghavachari, A. Rendell, J.C. Burant, S.S. Iyengar, J. Tomasi, M. Cossi, N. Rega, J.M. Millam, M. Klene, J.E. Knox, J.B. Cross, V. Bakken, C. Adamo, J. Jaramillo, R. Gomperts, R.E. Stratmann, O. Yazyev, A.J. Austin, R. Cammi, C. Pomelli, J.W. Ochterski, R.L. Martin, K. Morokuma, V.G. Zakrzewski, G.A. Voth, P. Salvador, J.J. Dannenberg, S. Dapprich, A.D. Daniels, Ö. Farkas, J.B. Foresman, J.V. Ortiz, J. Cioslowski, D.J. Fox. *Gaussian 09*. Gaussian, Inc., Wallingford, CT (2009).
19. R.F.W. Bader. Atoms in molecules. *Acc. Chem. Res.* **18**, 9 (1985).
20. S. Fliszar. *Charge Distributions and Chemical Effects* (Springer, 1983).
21. P. Politzer, P.R. Laurence, K. Jayasuria. Molecular electrostatic potentials: An effective tool for the elucidation of biochemical phenomena. *Environ. Health Perspect.* **61**, 191 (1985).
22. A. Jumabaev, S.J. Koyambo-Konzapa, H. Hushvaktov, A. Absanov, B. Khudaykulov *et al.* Intermolecular interactions in water and ethanol solution of ethyl acetate: Raman, DFT, MEP, FMO, AIM, NCI-RDG, ELF, and LOL analyses. *J. Mol. Model.* **30** (10), 349 (2024).
23. G. Job, F. Herrman. Chemical potential–a quantity in search of recognition. *Eur. J. Phys.* **27**, 353 (2006).
24. A. Jumabaev, B. Khudaykulov, U. Holikulov, A. Norkulov, J. Subbiah, O.M. Al-Dossary, N. Issaoui. Molecular structure, vibrational spectral assignments, MEP, HOMO-LUMO, AIM, NCI, RDG, ELF, LOL properties of acetophenone and for its solutions based on DFT calculations. *Opt. Mater.* **159**, 116683 (2025).
25. I. Rozas, I. Alkorta, J. Elguero. Behavior of Ylides containing N, O, and C atoms as hydrogen bond acceptors. *J. Am. Chem. Soc.* **122**, 11154 (2000).
26. E. Espinosa, E. Molins, C. Lecomte. Hydrogen bond strengths revealed by topological analyses of experimentally observed electron densities. *Chem. Phys. Lett.* **285**, 170 (1998).

Received 21.03.25

А. Жумабаєв, Х. Хушвактов,
А. Абсанов, Б. Худайкулов, У. Холікулов,
Л. Джуманов, Н. Іссауі, Л. Булавін

ЕКСПЕРИМЕНТАЛЬНЕ ТА ТЕОРЕТИЧНЕ ДОСЛІДЖЕННЯ МІЖМОЛЕКУЛЯРНИХ ВЗАЄМОДІЙ У НІТРОМЕТАНІ ТА ЙОГО РОЗЧИНАХ

У даній роботі обговорено коливальні (комбінаційного розсіювання світла та ІЧ) спектри нітрометану та його розчинів у полярних (хлороформ) та неполярних (чотирихлористий вуглець, гексан) розчинниках. Розглянуто геометричні параметри, розподіл заряду за Міллікеном, поверхню молекулярного електростатичного потенціалу та граничні молекулярні орбітальні комплекси нітрометану з молекулами хлороформу. $CH_3NO_2 + n \cdot CHCl_3$ (n = 1–3) на основі теорії функціонала густини (DFT) з базовим набором B3LYP/6-311++G(d,p). Слабкі молекулярні взаємодії в цих комплексах проаналізовано за допомогою методу Atoms in Molecule (AIM).

Ключові слова: нітрометан, спектри комбінаційного розсіювання, ІЧ спектри, водневий зв'язок, DFT, AIM.